The assembly state of the intermediate filament proteins desmin and glial fibrillary acidic protein at low ionic strength

Martin Kooijman[a,*], Herbert van Amerongen[a], Peter Traub[b], Rienk van Grondelle[a], Michael Bloemendal[c]

[a]*Department of Biophysics, Free University, De Boelelaan 1081, 1081 HV Amsterdam, The Netherlands*
[b]*Max Planck Institute for Cell Biology, D68526 Ladenburg/Heidelberg, Germany*
[c]*Department of Protein and Molecular Biology, Royal Free Hospital School of Medicine, Rowland Hill Street, London, NW3 2PF, UK*

Received 25 November 1994

Abstract The low ionic strength structures of the type III intermediate filament (IF) proteins desmin and glial fibrillary acidic protein (GFAP) have been studied by transient electric birefringence measurements. Flexible dimers with a length of around 45 nm, particles with a length of 68 ± 6 nm (presumably tetramers and hexamers) and larger aggregates of 108 ± 19 nm are found. GFAP has an increased tendency to aggregate upon lowering of the pH. The aggregation state of desmin does not change in the pH range studied. The results are compared with previous results on vimentin.

Key words: Intermediate filament protein; Desmin; Glial fibrillary acidic protein; Protein aggregation; Transient electric birefringence

1. Introduction

Intermediate filaments (IFs) are, together with microfilaments and microtubules, important constituents of the cytoskeleton. The various types of IF proteins differ considerably in molecular size and electric charge, but have a common basic molecular arrangement in the filaments. The central element is formed by two protein chains which form a coiled–coil structure of approximately 45 nm length, interrupted by a short linker region in the middle dividing the rod into two equally long parts (segments 1 and 2). The central rod domain is flanked by amino- and carboxy-terminal end domains, which are highly variable within the class of IF proteins.

These dimers are the simplest IF structures which can be found in aqueous solution of low ionic strength. Such structures are of interest, as they provide insight into the fundamentals of IF assemblage [1]. By increasing the ionic strength of the solution, higher IF aggregates can be induced. At the level of tetramers, basically two alignments of the constituting dimers have been proposed: an antiparallel in-register configuration (forming a structure of approximately 45 nm length [2,3]) and an antiparallel staggered (approximately 65 nm long) configuration [4–7]. Recently, we studied the structure of vimentin (a type III IF protein) and T-vimentin (vimentin missing the first 70 amino acids) by transient electric birefringence (TEB) measurements [8,9]. We have shown that, at low ionic strength and pH 6.0–10.2, T-vimentin is almost exclusively present as single dimers with a bent and/or flexible structure and a significant permanent dipole moment [9]. In solutions with 0.5 mM $MgCl_2$, antiparallel staggered tetrameric structures with a length of 63–68 nm and no permanent dipole moment were detected. It was concluded that most of these tetramers are rigid structures formed by overlap of the segment 1 regions of the constituting dimers (according to Steinert et al. [10]). A minor fraction might consist of slightly longer, but flexible/bent tetramers that show segment 2 overlap. For intact vimentin, particles with a length of about 65 nm and a relatively large permanent dipole moment were also observed [8]. These are most likely hexamers, as suggested by Steinert for keratin IF [5,6].

In order to determine the low ionic strength structures of two other type III IF proteins, we performed transient electric birefringence (TEB) (also called Kerr effect) measurements on glial fibrillary acidic protein (GFAP) and desmin. The first is present in astrocytes of the central nervous system and in cells of glial origin, while the latter is abundant in various types of muscle cells. Desmin resembles vimentin closely with respect to isoelectric point (pI 5.4) and size of the amino- and carboxy-end domains (approximately 100 and 55 residues, respectively) [11]. The pI of GFAP is slightly higher (pI 5.7), while the size of the amino end domain is considerably smaller (approximately 45 amino acids) than that of vimentin and desmin [12].

The field-free decay of the birefringence signal yields information that is directly related to the hydrodynamic properties of the complexes. In addition, information on their electric properties is obtained from comparison of the rise and decay of the TEB signals upon application of low-electric field pulses [13]. The data obtained for GFAP and desmin are compared to those of vimentin.

2. Materials and methods

2.1. Transient electric birefringence

The principles of the TEB measurements and the set-up used in this study have been described before [14]. The time constant of the electric birefringence set-up was 80 ns. For each birefringence curve at least 100 transients were averaged. Field strengths were determined by averaging 5 electric field pulses. The measurements were performed at 20°C. The following parameters were determined: (i) the ratio of the areas enclosed by the rise and decay curve of the birefringence, S_1/S_2 (see Fig. 1), which is related to the relative magnitudes of the permanent (P) and induced (Q) dipole moments according to [13]:

$$S_1/S_2 = (4P/Q + 1)/(P/Q + 1) \quad (1)$$

Note that $S_1/S_2 = 1$ in the absence of structures with a permanent dipole moment, and $S_1/S_2 = 4$ when a particle is exclusively oriented by a permanent dipole moment. (ii) The Kerr constant (K), which is defined as the proportionality constant between the magnitude of the

*Corresponding author. Fax: (31) (20) 444 7899.
E-mail: martink@nat.vu.nl

SSDI 0014-5793(94)01419-1

steady-state birefringence, Δn_0, and the square of the electric field E ($K = \Delta n_0/E^2$) at low field strengths. The Kerr constant is proportional to the product of the optical anisotropy factor and the sum of the dipole moments ($P + Q$) of the molecule. Δn_0 is determined by averaging the plateau of the rise curve. (iii) The field-free decay of the birefringence signal, yielding information on the hydrodynamic size of the molecules. In order to resolve multiple relaxation processes, the field-free decay times of the birefringence were analyzed on a SUN4 workstation using DISCRETE [15,16] and CONTIN [17,18]. The former is a program for the analysis of data in terms of discrete exponential decays, while the latter analyzes data in terms of a continuous distribution of exponential decay times. CONTIN and DISCRETE analyses were started 0.20 μs after the orienting field was turned off. When CONTIN and DISCRETE fits were started longer after the electric pulse, the values of the decay times did not vary, although the relative amplitudes of the shorter decay times decreased as compared to the longer ones. When relatively long electric field pulses (70–140 μs) were applied, a small contribution (< 5%) of a slow component was sometimes observed. The amplitude and decay time of this component were highly variable and dependent on the time window used for the analysis, whereas the relative contributions and decay times of the other components remained essentially unaltered upon variation of the time window. Therefore, we did not further consider this slow component. The solution of DISCRETE corresponding to the number of decay processes as determined by CONTIN was chosen, since the 'best solution' as given by DISCRETE does not always give reliable results [8,14,19,20].

In order to extract structural information from the relaxation times, we approximated the filament proteins as rigid cylindrical rods (see also [8,9]). For such particles the field-free decay time τ, as determined from birefringence decay data, equals $1/(6\theta)$, where θ is the rotational diffusion coefficient (s^{-1}). θ is related to the length (L) and diameter (d) of the cylinder by [21]:

$$\theta = \frac{3kT}{\eta_0 \pi L^3} \{\ln(L/d) - \gamma_R\} \quad (2)$$

$$\gamma_R = 0.877 - 7\left\{\frac{1}{\ln(2L/d)} - 0.28\right\}^2 \quad (3)$$

where η_0 is the viscosity of the sample, k is the Boltzmann constant, and T is the absolute temperature. The frictional parameter γ_R accounts for end effects. Note that θ depends strongly on L and much less on d.

2.2. Sample preparation

GFAP was purified from bovine brain white matter as described previously [22]. Desmin from chicken stomach was obtained from Boehringer-Mannheim. The lyophilized GFAP was dissolved in 2 mM phosphate buffer, pH 7.5, 6 mM 2-mercaptoethanol, 6 M urea, and dialyzed at 4°C for at least 16 h against 2 mM BisTris-HCl, pH 6.8, 6 mM 2-mercaptoethanol or 2 mM Tris-HCl, pH 8.5, 6 mM 2-mercaptoethanol. Desmin was dissolved in 10 mM phosphate buffer, pH 7.5, 1 mM EDTA, 2 mM dithiothreitol, 6 M urea, and dialyzed at 4°C against the same buffers as GFAP. The purity of GFAP was estimated to be >98% and of desmin >95%, based on SDS-PAGE. The final protein concentrations were determined by measuring the absorption at 280 nm (A_{280}). The molar extinction coefficient per protein chain at 280 nm was calculated from the extinction coefficient of the individual tryptophan ($\varepsilon = 6300$ $M^{-1} \cdot cm^{-1}$) and tyrosine residues ($\varepsilon = 1380$ $M^{-1} \cdot cm^{-1}$) [23]. These values are 20,000 $M^{-1} \cdot cm^{-1}$ for GFAP and 24,200 $M^{-1} \cdot cm^{-1}$ for desmin. In all TEB experiments, the protein concentration was between 0.05 and 0.15 mg/ml. Within this range all results were independent of protein concentration. Conductivity of the samples, determined by measuring the impedance of the solution in the Kerr cell at 1 kHz (Fluke Impedance Bridge Model 710B), was 300–400 Ω.

3. Results and discussion

The TEB of GFAP in 2 mM Tris, pH 8.5, is shown in Fig. 1. After a 70 μs pulse, steady-state birefringence is reached. The average field-free birefringence decay is strongly pulse-length dependent (not shown), which is indicative of size heterogeneity or flexibility/bending within the molecules [24]. When the field-free decay after a 70 μs pulse is analysed with CONTIN

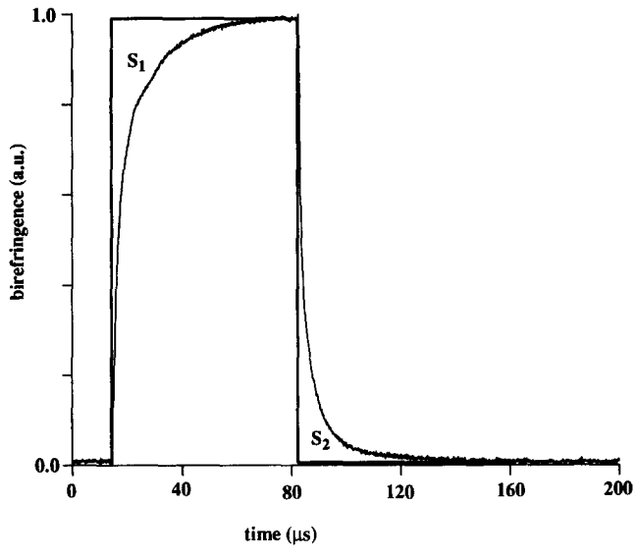

Fig. 1. Birefringence signal for GFAP in 2 mM Tris, pH 8.5. $E = 1.15$ kV/cm, pulse length 70 μs. S_1 and S_2 are the areas enclosed by the rise and decay curves, respectively (see text).

(Fig. 2) and DISCRETE (Table 1), three decay processes are obtained with relaxation times of around 0.5 μs, 2 μs and 5.5 μs (note that the x-axis of the CONTIN plots is logarithmic and that $1/\tau$ is given; thus, areas below the peaks do not correspond directly to relative contributions obtained from DISCRETE). A fourth CONTIN peak (Fig. 2 on the left) with a relative contribution of less than 5% corresponds to a very long relaxation time (> 30 μs). The position of this peak was highly sensitive to the starting point of the analysis and the time-range over which the fit was performed. For this reason, we do not take this long component into account (see also section 2).

The two shortest decay times are indicative for the presence of single dimers with a length of approximately 45 nm, as has been demonstrated in our recent TEB study on T-vimentin [9].

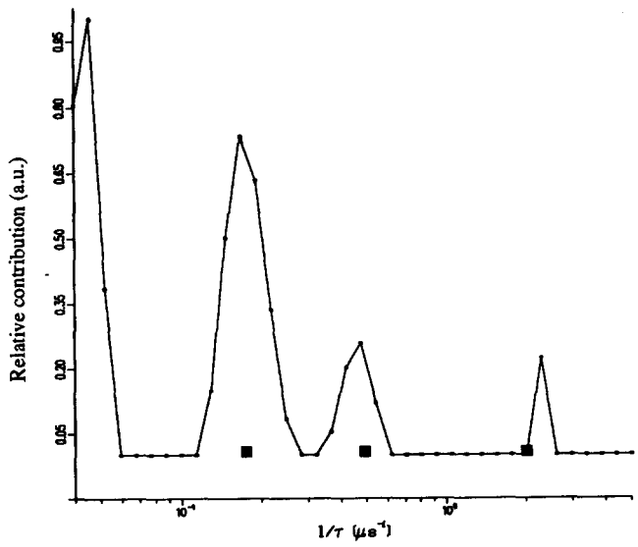

Fig. 2. Results from CONTIN (●) and DISCRETE (■) analyses of the birefringence decay of GFAP in 2 mM Tris, pH 8.5. Pulse duration 70 μs, $E = 1.15$ kV/cm.

The shortest decay time was attributed to bending or flexibility, the longer component to the end-over-end rotation of the dimers. For T-vimentin at pH values of 8.5 and 10.2, the relative contribution of the short component was 40%, and that of the longer one 60%. For GFAP at pH 8.5, in contrast, the shortest decay time contributes relatively more to the total TEB decay than the longer decay time (Table 1). Therefore, the shortest decay time is probably not exclusively due to bent and/or flexible dimers, and part of this component may be caused by some flexibility of larger aggregates. The third decay time corresponds to a cylinder length of 64–71 nm (according to Eqs. 2 and 3 with $d = 2.5$ nm, as found by Potschka et al. [4] for desmin tetramers), which is almost identical to that of staggered T-vimentin tetramers (63–68 nm) in the presence of 0.5 mM $MgCl_2$ [9]. For the fraction of those tetramers in which segments 2 of the constituting dimers overlap, we found a bent and/or flexible structure to be most likely. Assuming that such particles also occur in GFAP, the 'remainder' of the shortest decay time described above could be due to the flexible and/or bent structure of the latter. A S_1/S_2 value of 2.1 ± 0.5 for GFAP is observed, showing that at least part of the structures must possess a significant permanent dipole moment. Assuming the S_1/S_2 value of the dimers to be four (the theoretical maximum), the S_1/S_2 values belonging to τ_3 has to be 1.5 ± 0.7 in order to reach an overall value for S_1/S_2 of 2.1 ± 0.5 (for calculation, see [8]). Hence, although it is very likely that a fraction of the staggered particles has a permanent dipole moment (presumably hexamers, as pointed out in detail for vimentin [8]), it can not be ruled out that the observed S_1/S_2 value of 2.1 ± 0.5 is entirely due to single dimers (in the case when the S_1/S_2 value belonging to τ_3 is approximately 1).

For GFAP at pH 6.8, a decay time around 2 μs is not found even after pulses as short as 10 μs (see Fig. 3). Therefore, it is most likely that single dimers are absent at this pH and that the shortest decay time (0.7 ± 0.1) is due to a bent and/or flexible structure of some of the higher oligomers. The observed decay times for the staggered structures (τ_2 in Table 1) correspond to a length of 68 ± 6 nm ($d = 2.5$ nm). After steady-state pulses (140 μs), also longer structures with a decay time of 17 ± 4 μs are detected, which are probably higher order IF aggregates. When these are described as rigid rods with a diameter of 2.5 nm, their length would be 105 ± 9 nm (according to Eqs. 2 and 3). However, the presence of shorter particles with significantly increased diameter, or longer ones with bent and/or flexible structure, could also be responsible for the long decay time.

The increased aggregation state of GFAP at pH 6.8 may be due to the fact that the positive charge of the amino end domain is enhanced at this pH [25]. The importance of the charge of the amino end domain is illustrated by the fact that dephosphorylation of the head domain of GFAP (causing an increase of its positive charge) causes assembly of GFAP filaments [25].

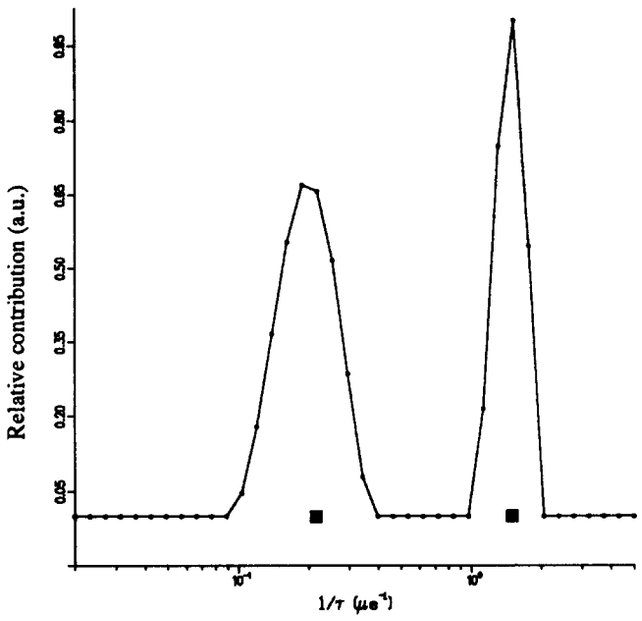

Fig. 3. Results from CONTIN (●) and DISCRETE (■) analyses of the birefringence decay of GFAP in 2 mM BisTris, pH 6.8. Pulse duration 10 μs, $E = 3.8$ kV/cm.

The aggregation state of desmin is not different at pH 8.5 and 6.8 (Table 1). At all pulse lengths, a relatively large contribution of decay times representing a staggered particle (τ_2 for 140 μs pulses and τ_3 after 5.0 μs pulses in Table 1) with a calculated length of 68 ± 6 nm ($d = 2.5$ nm) is observed. When short pulses of 5 μs are applied, decay components of 0.4 μs and approximately 1.8 μs, indicative of single dimers, are found. At steady-state pulses of 140 μs, both components merge into one average decay time of about 1.5 μs. This merging of decay times has been found before for vimentin [8]. Also decay times varying between 11 and 28 μs caused by larger aggregates (calculated length 108 ± 19 nm assuming $d = 2.5$ nm) are detected. As found for GFAP at pH 8.5, S_1/S_2 for desmin at pH 6.8 might be due to single dimers only, although the presence of a fraction of staggered particles with a permanent dipole moment (proba-

Table 1
TEB decay analysis (DISCRETE) for different pulse lengths; Kerr constants and S_1/S_2 values of GFAP and desmin at pH 6.8 and 8.5

IF protein	pH	Pulse length (μs)	S_1/S_2	A_1 (%)	τ_1 (μs)	A_2 (%)	τ_2 (μs)	A_3 (%)	τ_3 (μs)	K ($\times 10^{-13}$ $m^2 \cdot V^{-2}$) (per M monomer)
GFAP	8.5	70.0	2.1 ± 0.5	45 ± 10	0.5 ± 0.2	20 ± 7	2.0 ± 0.3	35 ± 17	5.5 ± 0.7	2.1 ± 0.5
GFAP	6.8	10.0	–	60 ± 5	0.7 ± 0.1	40 ± 5	4.8 ± 0.5	–	–	–
GFAP	6.8	140.0	1.5 ± 0.2	35 ± 5	1.0 ± 0.4	45 ± 5	6.0 ± 1.0	20 ± 10	17 ± 4	1.4 ± 0.3
Desmin	8.5	5.0	–	10 ± 5	0.4 ± 0.1	25 ± 10	1.7 ± 0.3	65 ± 15	5.5 ± 1.0	–
Desmin	8.5	140.0	2.2 ± 0.4	25 ± 5	1.5 ± 0.3	60 ± 7	6.0 ± 1.0	15 ± 12	18 ± 7	2.1 ± 0.4
Desmin	6.8	5.0	–	12 ± 7	0.4 ± 0.1	35 ± 5	2.0 ± 0.5	53 ± 12	6.0 ± 0.3	–
Desmin	6.8	140.0	1.6 ± 0.2	22 ± 8	1.6 ± 0.4	58 ± 4	5.9 ± 0.5	20 ± 12	24 ± 4	2.5 ± 0.3

bly hexamers) is more likely. At pH 8.5, however, the latter structures must be present in order to explain the relatively high S_1/S_2 value of 2.2 ± 0.4 (aggregates longer than 65 nm were shown to possess only an induced dipole moment (unpublished results)).

The Kerr constants of desmin and GFAP are in the same range as found before for vimentin and T-vimentin [8,9]. As these depend in a complicated way on size, charge and pH of the solution, we will not interpret the small differences in this paper.

4. Conclusions

4.1. The structure of type III IF proteins

Considerable fractions of the type III IF proteins desmin, GFAP (this study) and vimentin [8] at low ionic strength are present as staggered structures, most likely antiparallel tetramers with a length of approximately 66 ± 6 nm. In addition, a hexameric arrangement with a similar length but with a significant permanent dipole moment, and higher order IF aggregates with a length of 108 ± 19 nm, are likely to occur for these proteins. At pH 8.5, dimers are also found, which are bent and/or flexible structures with a length of approximately 45 nm. Therefore, single dimers seem to be the most elementary IF building blocks. For all IF proteins studied, the Kerr constants are of the same order of magnitude, also indicating comparable overall structures. The three IF proteins differ in their aggregation behaviour at different pH values: GFAP has an increased tendency to aggregate upon lowering the pH, in contrast to vimentin [8] which tends to aggregate to higher oligomers at higher pH values. Desmin aggregation does not change in the pH range studied. The different pH-dependent aggregation behaviours of the various IF proteins suggests that protein modifications affecting charge (like phosphorylation [25]) might be involved in regulation of IF assembly.

Acknowledgements: This work was supported by the Netherlands Organization of Scientific Research (NWO), in part via the Foundation of Biophysics and Biology (BION).

References

[1] Steinert, P.M. and Roop, D.R. (1988) Annu. Rev. Biochem. 57, 593–625.
[2] Ip, W., Hartzer, M.K., Pang, Y.-Y. and Robson, R.M. (1985) J. Mol. Biol. 183, 365–375.
[3] Quinlan, R.A., Hatzfeld, M., Franke, W.W., Lustig, A., Schulthess, T. and Engel, J. (1986) J. Mol. Biol. 192, 337–349.
[4] Potschka, M., Nave, R., Weber, K. and Geisler, N. (1990) Eur. J. Biochem. 190, 503–508.
[5] Steinert, P.M. (1991a) J. Struct. Biol. 107, 157–174.
[6] Steinert, P.M. (1991b) J. Struct. Biol. 107, 175–188.
[7] Geisler, N., Schünemann, J. and Weber, K. (1992) Eur. J. Biochem. 206, 841–852.
[8] Kooijman, M., Bloemendal, M., van Amerongen, H., Traub, P. and van Grondelle, R. (1994) J. Mol. Biol. 236, 1241–1249.
[9] Kooijman, M., Bloemendal, M., Traub, P., van Grondelle, R. and van Amerongen, H. (1994) J. Biol. Chem. (submitted).
[10] Steinert, P.M., Marekov, L.N. and Parry, D.A.D. (1993) J. Biol. Chem. 268, 24916–24925.
[11] Geisler, N. and Weber, K. (1982) EMBO J. 1, 1649–1656.
[12] Reeves, S.A., Helman, L.J., Allison, A. and Israel, M.A. (1989) Proc. Natl. Acad. Sci. USA 86, 5178–5182.
[13] Fredericq, E. and Houssier, C. (1973) in: Electric Dichroism and Electric Birefringence (Harrington, W. and Peacocke, A.R., eds.) chap. 1, Clarendon Press, Oxford.
[14] van Haeringen, B., Jiskoot, W., van Grondelle, R. and Bloemendal, M. (1992) J. Biol. Struct. Dyn. 9, 991–1011.
[15] Provencher, S.W. (1976a) Biophys. J. 16, 27–41.
[16] Provencher, S.W. (1976b) J. Chem. Phys. 64, 2772–2777.
[17] Provencher, S.W. (1982a) Comp. Phys. Commun. 27, 213–227.
[18] Provencher, S.W. (1982b) Comp. Phys. Commun. 27, 229–242.
[19] Highsmith, S. and Eden, D. (1986) Biochemistry 25, 2237–2242.
[20] Lewis, R.J., Pecora, R. and Eden, D. (1986) Macromolecules 19, 134–139.
[21] Broersma, S. (1960) J. Chem. Phys. 32, 1626–1631.
[22] Vorgias, C.E. and Traub, P. (1983) Biochem. Biophys. Res. Commun. 115, 68–75.
[23] Weast, R.C. (1971) Handbook of Chemistry and Physics (52th edition) The Chemical Rubber Co., Cleveland, OH.
[24] Curry, J.F. and Krause, S. (1991) Biopolymers 31, 1677–1687.
[25] Inagaki, M., Gonda, Y., Nishizawa, K., Kitamura, S., Sato, C., Ando, S., Tanabe, K., Kikuchi, K., Tsuiki, S. and Nishi, Y. (1990) J. Biol. Chem. 265, 4722–4729.